Main Group Met. Chem. 2019; 42: 8–12 **DE GRUYTER**

Kun-Ning Yang, Ke-De Yuan, Li-Li Jiang and Yong Zhang*

A new Pb(II)-based coordination polymer constructed from a semirigid tricarboxylate ligand: crystal structure and anti-lung cancer activity

https://doi.org/10.1515/mgmc-2018-0034
Received June 21, 2018; accepted October 19, 2018

Abstract: Based on a semirigid tricarboxylate ligand 5-((4-carboxyphenoxy)methyl)benzene-1,3-dioic acid (H_3L), a new Pb(II)-based coordination polymer formulated as $[Pb(HL)(H_2O)](H_2O)$ (**1**) was synthesized under solvothermal conditions and characterized by single-crystal X-ray structural analysis, power X-ray diffraction, and elemental analysis. Compound **1** is a two-dimensional layered structure formed by the connection of the one-dimensional Pb(II)-based secondary building unit chains with the partly deprotonated HL ligands, which are further extended into three-dimensional supermolecular structures through the H-bonds. Furthermore, the size of the as-prepared **1** could be downsized into the nano region through a simple ultrasonic method. Finally, the anti-lung cancer activities of **1** and the nanosized **1** have been probed via the MTT assay against three human lung cancer cell lines (A549, H1299, and PC9).

Keywords: cancer cell; Pb(II)-coordination polymer; X-ray diffraction.

Introduction

The coordination complexes cisplatin and carboplatin have a wide range of applications in cancer chemotherapy (Cheng et al., 2018). Testicular, ovarian, and bladder cancer have been treated successfully by combinations containing these and other antitumor drugs (Zhao et al., 2018). Also, small-cell lung cancer has been shown to be responsive to platinum chemotherapy. However, the high cost, obvious side effect, and low cell selectivity of these Pt-based drugs encourage scientists to search for more effective coordination-based drugs for cancer treatment (Hall et al., 2008).

The field of infinite coordination polymer particles is rapidly growing due to their potential use in a variety of important applications. These structures, which consist of repeating ligands interconnected by metallic nodes, are appealing because they can be made from readily available and highly tailorable metal and ligand precursors, often have chemically adjustable porosities and high internal surface areas, and provide the researcher with a network structure that can be deliberately and easily modified for many applications, including catalysis, gas storage, separations, photonics, and biomedical fields (Collins and Zhou, 2007; Cadiau and Brites, 2013; Chen et al., 2015; Li et al., 2017; Qu and Li, 2017; Li and Li, 2018). To this end, hundreds of new coordination polymers have been made over the past decade. Because of the versatile coordination modes, aromatic carboxylate linkers are most used to construct coordination polymers, and the typical example is using rigid linear dicarboxylate acids of various lengths to construct a family of isoreticular coordination polymers with **pcu** topology based on Zn_4O-based secondary building unit (SBUs) (Zhou et al., 2018). Compared with rigid aromatic ligands, flexible multicarboxylate linkers enable the formation of frameworks with uncommon or even novel topologies and special properties because of their flexibility and conformational diversity (Zang et al., 2006). It is obvious that the use of flexible linkers presents a direct approach toward the understanding of the structure–property relationship of coordination polymers. In this study, 5-((4-carboxyphenoxy)methyl)benzene-1,3-dioic acid (H_3L, Figure 1), a Y-shaped tricarboxylic acid, was chosen as the primary ligand. It can provide various coordination sites and may form fascinating structures with intriguing topologies. For instance, He and coworkers report two new Co(II)-based coordination polymers based on the H_3L ligand, which shows two-fold interpenetrating **hms** framework or three-dimensional (3D) **pcu** net depending on the reaction conditions used (He et al., 2017a,b). In that same year, the author used the H_3L and 4,4′-bipyridine to construct a mixed-ligand Zn(II)-based coordination polymer, which could be used as a luminescent sensor for Fe^{3+} ion with high selectivity and sensitivity (He et al., 2017a,b). However, to the best of our knowledge, there are no reports

---

***Corresponding author: Yong Zhang,** Respiratory and Critical Care Medicine, Weifang Respiratory Disease Hospital (Weifang No. 2 People's Hospital), Weifang 261041, Shandong, China, e-mail: yong_zhang666@126.com
Kun-Ning Yang, Ke-De Yuan and Li-Li Jiang: Respiratory and Critical Care Medicine, Weifang Respiratory Disease Hospital (Weifang No. 2 People's Hospital), Weifang 261041, Shandong, China

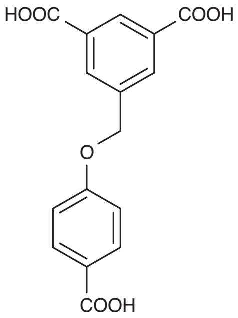

Figure 1: Chemical structure of the H_3L ligand used in this work.

of main group metal-based coordination polymer based on the H_3L ligand. In this work, a new Pb(II)-based coordination polymer formulated as $[Pb(HL)(H_2O)](H_2O)$ (**1**) was synthesized under solvothermal conditions and characterized by single-crystal X-ray structural, power X-ray diffraction, and elemental analysis (EA). Compound **1** is a two-dimensional (2D) layered structure that is formed by the connection of the one-dimensional (1D) Pb(II)-based SBU chains with the partly deprotonated HL ligands, which are further extended into 3D supermolecular structures through the H-bonds. Furthermore, the size of the as-prepared **1** could be downsized into the nano region through a simple ultrasonic method. Finally, the anti-lung cancer activities of **1** and the nanosized **1** have been probed through the MTT assay against three human lung cancer cell lines (A549, H1299, and PC9).

Results and discussion

Structural analysis

Structural analysis for **1** using X-ray single-crystal diffraction reveals that the framework of **1** with the chemical formula of $[Pb(HL)(H_2O)](H_2O)$ belongs to the triclinic space group $P\bar{1}$ and is built up from the 1D chain-like SBU. The molecular building unit of **1** contains one Pb(II) ion, one partly deprotonated HL ligand, one coordinated water, and one lattice water molecule. As shown in Figure 2A, the coordination surrounding the Pb(II) ion is completed by five carboxylic O atoms from four different HL ligands, and the remaining site is finished by the coordinated water molecule, shaping a bicapped seesaw coordination geometry. The Pb(II)-O bond lengths vary from 2.492(5) to 2.659(3) Å, and these bond distances are comparable with those of the Pb(II)-based coordination polymers in

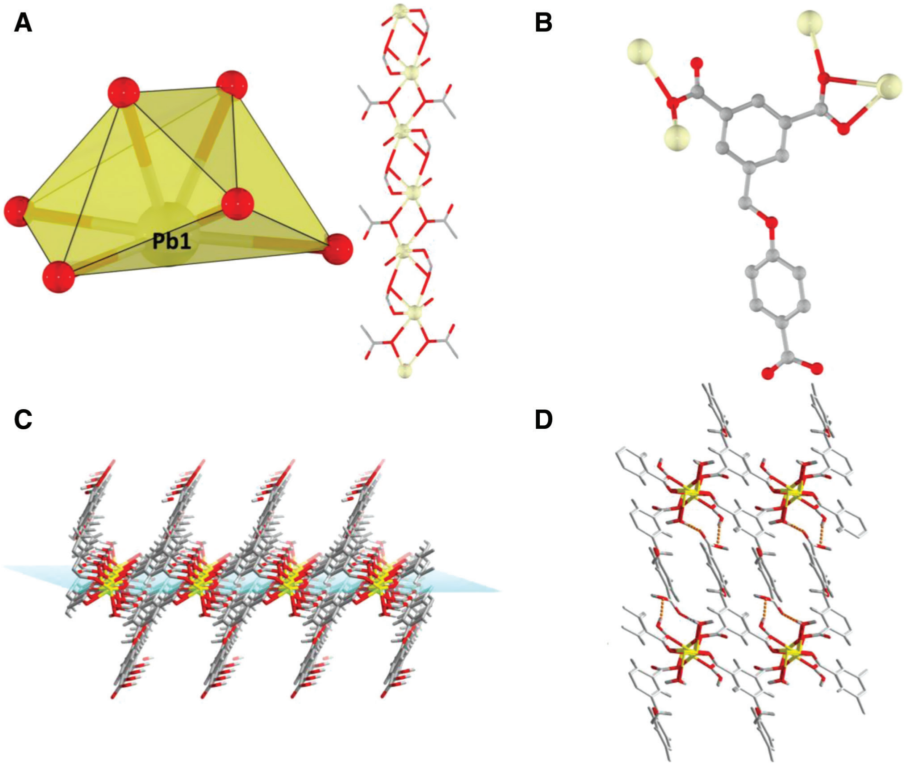

Figure 2: The crystal structures for compound **1**.
(A) View for the coordination surrounding of the Pb(II) ion; (B) view for the connection modal for the HL ligand; (C) the 2D layered network of **1**; (D) the 3D supermolecular framework of **1** formed by the H-bond interactions.

the literature (Yang et al., 2007; Li et al., 2010; Che et al., 2011). For the complex **1**, there is an obvious gap in the coordination spheres of Pb(II) ions, for example, the bond angle for O2-Pb1-O3 is 154.69(4)°, which indicates the stereochemical activity of the lone pair of electrons. The adjacent Pb(II) ions are held together by four carboxylic groups along the *b* axis to afford the 1D chain-like SBU with the nearest Pb(II)-Pb(II) distance of 4.200(4) Å. In the structure of **1**, the HL linkers are arranged in the crystallographic inversion center binding with four Pb(II) ions and two Pb(II)-chains, in which the two carboxylate groups adopt a μ_2–η^2:η^1 and μ_2–η^2 bridging modes (Figure 2B). The Pb(II) chains are held together by the HL linkers along the *ab* plane to afford the 2D layered network with the uncoordinated carboxylic groups pointing outside of the *ab* plane (Figure 2C). PLATON analysis reveals that complex **1** holds a solvent accessible void of 3.4%, which is occupied by the lattice water molecules. The adjacent 2D layers are further extended into 3D supermolecular structure through the H-bonds between the coordinated water molecule and the undeprotonated carboxylic groups on the HL ligand with a short O···H-O distance of 1.842(3) Å (Figure 2D).

To check the purity and homogeneity of the bulk products of **1**, the as-synthesized samples of **1** were measured by X-ray powder diffraction at room temperature. As shown in Figure 3A, the peak positions of the experimental patterns are in good agreement with the simulated ones, which clearly indicate the good purity and homogeneity of the compounds. Figure 3B shows the nanoflower that was observed using scanning electron microscope (SEM). The morphology of compound **1**, prepared using the sonochemical method, is very interesting. It is composed of cross-sheets with a thickness of approximately 40–50 nm. The mechanism of formation of these structures needs to be further investigated. However, it may be a result of the crystal structure of a compound that is a supramolecular structure, i.e. the packing of the structure on a molecular level might have influenced the morphology of the nanostructure of the compound.

In vitro cytotoxicity study against the tumor cells

To preliminary access the anticancer efficacies of the two complexes (**1** and nano-**1**), their tumor cell growth inhibition activity against human lung cancer cell lines (A549, H1299, and PC9) was evaluated by MTT cell viability assay with doxorubicin as the reference drug. Exposure time was set to 48 h and the cell growth inhibition activity effects of cisplatin were used to make a comparison with the results of the title complexes. Dimethyl sulfoxide was used to dissolve the compounds at a concentration of 1 μM, and the diluted solution was added into the cell culture.

The data, which represent mean ± SEM of three independent tests carried out in duplicate, were plotted in Figure 4A. A descending order could be observed for the antiproliferative activity of the test complexes toward each type of the tumor cell lines used, which might be ascribed to the measured concentration required to inhibit tumor cell proliferation by 50% (IC_{50} μ/M). From the results above, we can conclude that the newly prepared nano-**1** demonstrate comparable growth inhibition activity toward all three types of cancer cells with the reference drug doxorubicin, indicating their potential use as antitumor drugs. Furthermore, these results also show that the anticancer activities of **1** are greatly enhanced by downsizing into the nanoscale region. To explore the low cytotoxicity of nano-**1** *in vitro*, oral epidermal cells (normal cells) were chosen to incubate with nano-**1** under different concentrations (0–80 μg/mL) for 24 h. As shown in Figure 4B, the cell

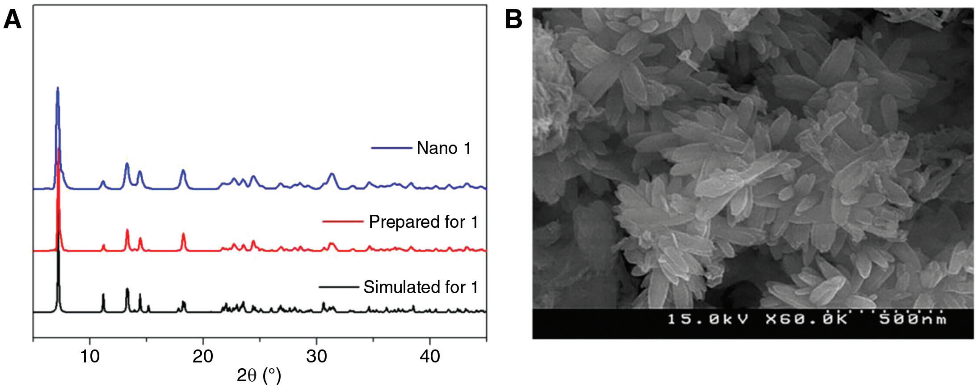

Figure 3: The PXRD pattern and SEM image for compound **1**.
(A) The simulated and experimental X-ray powder diffraction curves for complex **1**; (B) the SEM image of nano-**1**.

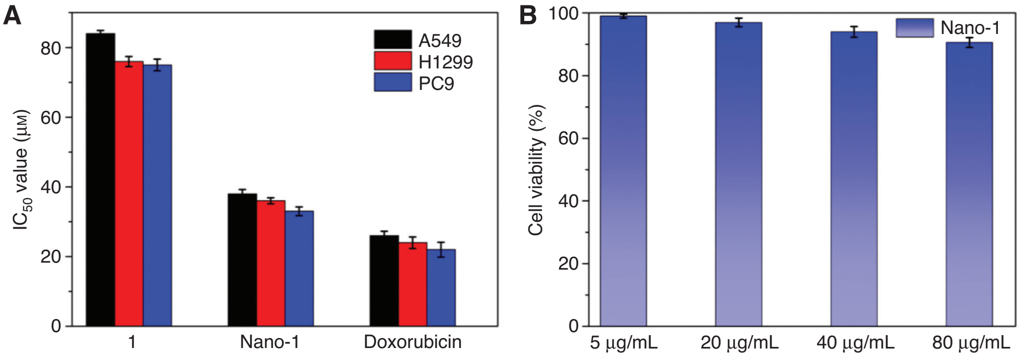

Figure 4: The MTT assay results for compound **1**.
(A) The IC_{50} value of the two metal–organic complexes and doxorubicin against A549, H1299, and PC9; (B) cell viabilities of the oral epidermal cells after incubation with nano-**1** at different concentrations for 24 h.

viabilities all remained at more than 85% even at a concentration of 80 μg/mL of nano-**1**; therefore, the nano-**1** showed low cytotoxicity in the oral epidermal cells.

Conclusion

In summary, a new Pb(II)-based coordination polymer formulated as $[Pb(HL)(H_2O)](H_2O)$ (**1**) was synthesized using a semirigid tricarboxylate ligand 5-((4-carboxyphenoxy) methyl)benzene-1,3-dioic acid. Furthermore, the size of the as-prepared **1** could be controlled in the nanoscale region through a simple one-pot solvothermal reaction with the aid of ultrasonic treatment. In connecting to their structures, the MTT assay indicates the obvious antitumor activities for compound nano-**1** against human lung cancer cell lines (A549, H1299, and PC9).

Experimental

Reagents and general methods

The chemicals in this work were bought from Bailingwei Reagent Company (Beijing, China) and used as-received. The H3L ligand was obtained from Shangdong Freda Biopharm Co., Ltd. (Jinan, China). An elemental analyzer (Perkin-Elmer 2400C; Waltham, MA, USA) was used to obtain the C, H, and N contents of the two coordination compounds. Cu Kα radiation equipped Bruker D8-ADVANCE (Bruker AXS, Karlsruhe, Germany) was used to collect the power X-ray diffraction curves. A ST-4800 (Hitachi, Tokyo, Japan) SEM was used to determine the morphology of the nano-sized **1**.

Preparation methods for compound $[Pb(HL)(H_2O)](H_2O)$ (1)

A mixture of H_3L (32 mg, 0.1 mmol), bpy (8 mg, 0.05 mmol), $Pb(CH_3COO)_2$ (32 mg, 0.1 mmol), 2 mL DMF, and 6 mL water was sealed in a 15 mL Teflon reactor and heated at 120°C for 72 h. After cooling to ambient temperature, colorless crystals of **1** were obtained in 65% yield. Anal. Calc. for $C_{16}H_{14}O_9Pb$ ($M_r = 557.48$): C, 34.47; H, 2.53. Found: C, 34.21; H, 2.80. IR (cm^{-1}): 3063(*s*), 1604(*w*), 1511(*w*), 1455(*w*), 1410(*m*), 1380(*m*), 1314(*m*), 1161(*m*), 1124(*s*), 1101(*s*), 1071(*m*), 927(*s*), 850(*m*), 791(*s*).

Preparation of nano-**1**: a solution of $Pb(CH_3COO)_2 \cdot$ in H_2O (15 mL, 0.01 M) was placed in a high-density ultrasonic probe, operating at 20 kHz with a maximum power output of 600 W. To this solution, a solution of the ligand H_3L (32 mg, 0.1 mmol) was added dropwise. The obtained precipitates were filtered off, washed with water, and dried in air.

X-ray single crystal structure determination

An Oxford Xcalibur E diffractometer (Oxford Instruments, Oxford, UK) with graphite monochromatized Mo Kα radiation (0.71073 Å) was used to collect the reflection data of **1** at 298 K. The direct method in the XS program was used to obtain the initial structural modes, and the least-squares method in XL program was used to refine the structural models (Sheldrick, 2015). All the H atoms were generated at their ideal locations and refined using the AFIX commands according to their C atoms attached, and all nonhydrogen atoms in the two structures were treated anisotropically. The solvent information of **1** and **2** were obtained from the EA results. Table 1 shows the crystal data and the structure refinement parameter.

Antitumor activity

A549, H1299, and PC9 human lung cancer cell lines were developed in an RPMI 1460 medium supplemented with 10% fetal calf serum, 0.1 g/L streptomycin, and 0.1 g/L penicillin. The above systems were incubated in a humidified incubator with air and CO_2 (95:5, v/v) at 37°C. The RPMI 1640 was used to dilute the cells to a concentration of 5×10^4 cells/mL. The 96-well cell culture at a volume of 100 μL per cell was used to seed the cells. Then, the system was incubated at 37°C under humidified CO_2 (5%) surroundings for 1 day. The cells were treated with each complex for 1 day, then the crystals were removed and the MTT solution (0.5 mg/mL, 150 μL) was added to each well tested and the plates were cultured for 4 h. Afterward,

Table 1: Crystallographic data and refinement parameters for complex **1**.

Formula	$C_{16}H_{14}O_9Pb$
M_r	557.46
Crystal system	Triclinic
Space group	$P\bar{1}$
a/Å	8.1769 (8)
b/Å	8.3756 (9)
c/Å	12.8647 (12)
α/°	72.805 (2)
β/°	86.282 (2)
γ/°	75.708 (2)
V/Å^3	815.60 (14)
Z	2
D_{calc}/g · cm^{-3}	2.270
μ(Mo Kα)/mm^{-1}	10.394
θ range/°	1.657–25.006
Reflections collected	5944
No. unique data [R(int)]	2824 [0.0292]
No. data with $I \geq 2\sigma(I)$	2662
R_1 ($I \geq 2\sigma(I)$)	0.0426
ωR_2(all data)	0.1296
CCDC	1850907

100 μL of dimethyl sulfoxide was transferred into each well to dissolve the samples after the MTT-containing media were removed. A microplate reader (Perkin-Elmer) was used to record the absorbance at a wavelength of 450 nm, which is further used in the calculation of the cell relative viability. Each parallel experiment was carried out at least three times to obtain the mean values. The value for the cell viability was calculated using absorbance peak at 540 nm.

References

Cadiau, A.; Brites, C. D. S.; Costa, P. M. F. J.; Ferreira, R. A. S.; Rocha, J.; Carlos, L. D. Ratiometric. Nanothermometer based on an emissive Ln^{3+}-organic framework. *ACS Nano.* **2013**, *7*, 7213–7218.

Che, G. B.; Chen, J.; Wang, X. C.; Liu, C. B.; Wang, C. J.; Wang, S. T.; Yan, Y. S. A novel pillared double-layered Pb(II) coordination polymer based on 1,3,5-benzenetricarboxylic acid and dipyrido[3,2-a:2′,3′-c]-phenazine-2-carboxylic acid. *Inorg. Chem. Commun.* **2011**, *14*, 1086–1088.

Chen, D.; Shi, W.; Cheng, P. A cage-based cationic body-centered tetragonal metal–organic framework: single-crystal to single-crystal transformation and selective uptake of organic dyes. *Chem. Commun.* **2015**, *51*, 370–372.

Cheng, Q.; Li, X.; Wang, Y.; Dong, M.; Zhan, F. H.; Liu, J. The ceramide pathway is involved in the survival, apoptosis and exosome functions of human multiple myeloma cells in vitro. *Acta Pharmacol. Sin.* **2018**, *39*, 561–568.

Collins, D. J.; Zhou, H. C. Hydrogen storage in metal–organic frameworks. *J. Mater. Chem.* **2007**, *17*, 3154.

Hall, M. D.; Okabe, M.; Shen, D. W.; Liang, X. J.; Gottesman, M. M. The role of cellular accumulation in determining sensitivity to platinum-based chemotherapy. *Annu. Rev. Pharmacol. Toxicol.* **2008**, *48*, 495–535.

He, Y. C.; Xu, N.; Zhao, F. H.; Kan, W. Q.; Liu, H. R.; You, J. Two novel Co(II)-based coordination polymers with. Hms and Pcu nets: syntheses, structures and properties. *Inorg. Chem. Commun.* **2017a**, *86*, 78–81.

He, Y. C.; Xu, N.; Zhao, F. H.; Kan, W. Q.; Wang, Y.; You, J. A luminescent Zn(II)-based coordination polymer constructed by 5-((4-carboxyphenoxy)methyl)benzene-1,3-dioic acid and 4,4′-bipyridine for selective sensing of Fe^{3+}. *Polyhedron* **2017b**, *134*, 330–335.

Li, J.; Li, J. T. A luminescent porous metal–organic framework with Lewis basic pyridyl sites as a fluorescent chemosensor for TNP detection. *Inorg. Chem. Commun.* **2018**, *89*, 51–54.

Li, D. S.; Wu, Y. P.; Zhang, P.; Du, M.; Zhao, J.; Li, C. P.; Wang, Y. Y. An unprecedented eight-connected self-penetrating coordination framework based on cage-shaped [Pb$_6$(μ$_4$-O)$_2$(O$_2$C)$_8$] clusters. *Cryst. Growth Des.* **2010**, *10*, 2037–2040.

Li, J.; Ji, X. H.; Li, J. T. Two new inorganic anions directed Zn(II)-tetrazole frameworks: syntheses, structures and. photoluminescent properties. *J. Mol. Struct.* **2017**, *1147*, 22–25.

Qu, Y. J.; Li, J. A water-stable La-based coordination polymer for highly fluorescent detection of Fe^{3+} ion and nitrobenzene vapor. *Inorg. Chem. Commun.* **2017**, *76*, 77–80.

Sheldrick, G. M. Crystal structure refinement with SHELXL. *Acta Crystallogr. C Struct. Chem.* **2015**, *71*, 3–8.

Yang, J.; Li, G. D.; Cao, J. J.; Yue, Q.; Li, G. H.; Chen, J. S. Structural variation from 1D to 3D: effects of ligands. and solvents on the construction of lead(II)–organic coordination polymers. *Chem.-A Eur. J.* **2007**, *13*, 3248–3261.

Zang, S.; Su, Y.; Li, Y.; Ni, Z.; Meng, Q. Assemblies of a new flexible multicarboxylate ligand and D10 metal centers toward the construction of homochiral helical coordination polymers: structures, luminescence, and NLO-active properties. *Inorg. Chem.* **2006**, *45*, 174–180.

Zhao, C.; Liu, G.; Li, X.; Guan, Y.; Wang, Y.; Yuan, X.; Sun, G.; Wang, Z.; Li, X. Inflammatory mechanism of rumenitis in dairy cows with subacute ruminal acidosis. *BMC Vet. Res.* **2018**, *14*:135.

Zhou, H. F.; Liu, B.; Hou, L.; Zhang, W. Y.; Wang, Y. Y. rational construction of a stable Zn4O-based MOF for highly efficient CO$_2$ capture and conversion. *Chem. Commun.* **2018**, *54*, 456–459.